Transportation Research Part D 34 (2015) 137–154

Contents lists available at ScienceDirect

Transportation Research Part D

journal homepage: www.elsevier.com/locate/trd

Atmospheric dispersion modeling near a roadway under calm meteorological conditions

Masoud Fallah Shorshani [a,c,*], Christian Seigneur [a], Lucie Polo Rehn [b,c], Hervé Chanut [d], Yann Pellan [d], Jean-luc Jaffrezo [b], Aurélie Charron [c], Michel André [c]

[a] CEREA, Joint Laboratory École des Ponts ParisTech/EDF R&D, Université Paris-Est, 77455 Marne-la-Vallée Cedex 2, France
[b] Univ. Grenoble Alpes, CNRS, LGGE, UMR5183, F-38000 Grenoble, France
[c] IFSTTAR Institut Français des Sciences et Technologies des Transports, de l'Aménagement et des Réseaux, 69675 Bron Cedex, France
[d] Air Rhône-Alpes, F-69500 Bron, France

ARTICLE INFO

Keywords:
Gaussian plume model
Calm meteorological conditions
On-road traffic emissions
Emission model
Metal concentrations
PM resuspension

ABSTRACT

Atmospheric pollutant dispersion near sources is typically simulated by Gaussian models because of their efficient compromise between reasonable accuracy and manageable computational time. However, the standard Gaussian dispersion formula applies downwind of a source under advective conditions with a well-defined wind direction and cannot calculate air pollutant concentrations under calm conditions with fluctuating wind direction and/or upwind of the emission source. Attempts have been made to address atmospheric dispersion under such conditions. This work evaluates the performance of standard and modified Gaussian plume models using measurements of NO_2, PM_{10}, $PM_{2.5}$, five inorganic ions and seven metals conducted near a freeway in Grenoble, France, during 11–27 September 2011. The formulation for calm conditions significantly improves model performance. However, it appears that atmospheric dispersion due to vehicle-induced turbulence is still underestimated. Furthermore, model performance is poor for particulate species unless road dust resuspension by traffic is explicitly taken into account.

Introduction

Studies have shown that populations spending large amounts of time near major roadways have an increased incidence and severity of health problems that may be related to air pollution from roadway traffic (Baldauf et al., 2008). Health effects include reduced and impaired lung function, asthma and other respiratory symptoms, cardiovascular effects, low birth weight, cancer, and premature death (e.g., Garshick et al., 2003; Janssen et al., 2002; Gauderman et al., 2005; Heinrich et al., 2005; McConnell et al., 2006; Pirjola et al., 2006). Therefore, it is essential to estimate population exposure near roadways in support of exposure and epidemiological studies as well as for impact studies of future roadway projects. To that end, one needs to select traffic, emission, and air quality models relevant to the given case study. Traffic models can be classified as static or dynamic models according to spatio-temporal scales. However, in many studies, traffic data are

* Corresponding author at: CEREA, Joint Laboratory École des Ponts ParisTech/EDF R&D, Université Paris-Est, 6–8 av. Blaise Pascal, Cité Descartes, Champs-sur-Marne, 77455 Marne-la-Vallée Cedex 2, France.

E-mail addresses: masoud.fallah@cerea.enpc.fr (M. Fallah Shorshani), seigneur@cerea.enpc.fr (C. Seigneur), Lucie.Polo@lgge.obs.ujf-grenoble.fr (L. Polo Rehn), Hchanut@air-rhonealpes.fr (H. Chanut), YPellan@air-rhonealpes.fr (Y. Pellan), Jean-luc.Jaffrezo@lgge.obs.ujf-grenoble.fr (J.-l. Jaffrezo), aurelie.charron@ifsttar.fr (A. Charron), michel.andre@ifsttar.fr (M. André).

http://dx.doi.org/10.1016/j.trd.2014.10.013
1361-9209/

available from measurements that can be used directly as inputs for emission models. Emission models use traffic data (fleet composition, vehicle speed, etc.) and other relevant data (e.g., road gradient, ambient temperature) to estimate traffic-related emissions of air pollutants, which are used as inputs to an atmospheric dispersion model. A variety of atmospheric dispersion models are available to simulate the concentrations of air pollutants as a function of time and space, with different levels of details (Holmes and Morawska, 2006; Zannetti, 1990; Sportisse, 2009). Eulerian and Lagrangian models are typically used for large domains, ranging from urban to global scales. At local scales (i.e., near emission sources), different models are used depending on topography. Gaussian dispersion models are typically used for cases without obstacles or with obstacles of simple geometry. Street-canyon models may be appropriate for cities with high buildings, although for cases with complex geometries computational fluid dynamics (CFD) models may be required.

In this work, we use a Gaussian dispersion model to simulate air pollutant concentrations near a roadway. Actual traffic data are used as input to estimate air pollutant emissions. Concentrations of pollutants were measured near the roadway for a two-week period. Local meteorological measurements were also available. During that period, wind speeds were mostly low and the prevailing wind direction was such that the measurement site was located mostly upwind of the roadway. Most Gaussian dispersion models are designed for receptors located downwind of the roadway and for conditions with a significant wind speed (Benson, 1989; Zhang and Batterman, 2010; Kenty et al., 2007). However, conditions with calm meteorological conditions and upwind locations are also relevant to population exposure. Therefore, this study examines the performance of a Gaussian model with and without modification for calm meteorological conditions using the measurements conducted near a roadway. First, the formulation of the atmospheric dispersion model is briefly presented. Then, the field campaign is described. Finally, the model simulation results are presented and discussed.

Model description

The emission and atmospheric dispersion models must be selected such that they are consistent in terms of level of detail, input requirements, and spatial and temporal resolution. An emission model based on average vehicle speed is appropriate here considering the available traffic data.

Two steady-state models are used here to simulate the atmospheric dispersion of pollutants: a Gaussian plume model for roadway sources (Briant et al., 2011, 2013) and this plume model augmented with a formulation suitable for conditions with light winds (Venkatram et al., 2013).

Gaussian plume formulation for roadway sources

The Gaussian dispersion model used here for the atmospheric dispersion of pollutants emitted from a roadway is that of Briant et al. (2011, 2013). The concentration field is calculated with an equation that minimizes the error when the wind direction is not perpendicular to the roadway:

$$C_p(x,y,z) = \frac{qF(z)}{2\sqrt{2\pi}u\cos\theta\sigma_z(d_{eff})} \times [erf(t_1) - erf(t_2)] \times \left(\frac{1}{L(x_{wind})+1}\right) + E(x_{wind}, y_{wind}, z) \quad (1)$$

where, $t_i = \frac{(y-y_i)\cos\theta - x\sin\theta}{\sqrt{2}\sigma_y(d_i)}$; $F(z) = \left(\exp\left(-\frac{(h_s-z)^2}{2\sigma_z^2}\right) + \exp\left(-\frac{(h_s+z)^2}{2\sigma_z^2}\right)\right)$; $d_{eff} = \frac{x}{\cos\theta}$; $d_i = (x - x_i)\cos\theta + (y - y_i)\sin\theta$.

C is the pollutant concentration in g m^{-3} at the location of the receptor (x, y, z), x is the distance from the source along the wind direction in m, y and z are the cross-wind distances from the plume centerline in m, x_i and y_i are the coordinates of the source (road segment) extremities, u is the wind velocity in m s^{-1}, q is the emission rate per unit length of the line source in g m^{-1} s^{-1}, and σ_y and σ_z are the standard deviations representing pollutant dispersion in the cross-wind directions in m. L and E are analytical functions that minimize the error when the wind direction is not perpendicular to the line source. The standard deviations σ_y and σ_z are computed here with the Briggs parameterization (Briggs, 1973). The effective distance d_{eff} is used to compute σ_z and d_i is the distance from each extremity of the line source section in the wind direction used to compute σ_y. This equation applies when the angle θ between the wind direction and the normal to the road segment ranges from 0° to 80°.

When the wind is parallel or nearly parallel (80° $\leqslant \theta \leqslant$ 90°) to the roadway, the concentration, C, is calculated as a combination between Eq. (1) and a numerical solution ($C_{\text{discretized}}$) obtained by discretizing the line source as a series of point sources:

$$C = (1-\alpha)C_p + \alpha C_{\text{discretized}} \quad (2)$$

The coefficient α varies linearly from 0 to 1 when θ vary from 80° to 90°.

This model was successfully evaluated against a reference solution as well as against observations obtained over a large road network in France (Briant et al., 2013). The overall spatial correlations for nitrogen dioxide (NO_2) concentrations measured and modeled at 242 sites were between 0.74 and 0.79, which indicates that the model explains more than half of the spatial variability observed in the monthly-averaged observations. Although the results for spatial variability were satisfactory, the ability of the model to reproduce temporal variability could not be evaluated in this previous work (Briant et al., 2013) because of a lack of hourly-averaged data. However, the temporal correlations between observed and modeled concentrations are typically poor for many models. For example Misra et al. (2013) obtained a correlation of hourly nitrogen oxides (NO_x) simulated concentrations with the Gaussian model AERMOD of 0.35. Hirtl and Baumann-Stanzer (2007) simulated NO_x concentration with the Gaussian model ADMS-Roads. They showed that point-to-point comparisons of measured and modeled concentrations paired in space and time (hourly) usually result in a very weak correlation. A variety of statistical metrics may be used to evaluate model performance. Several studies (Qian and Venkatram, 2011; Venkatram et al., 2013; Chang and Hanna, 2004) used the fraction of the modeled concentrations that are within a factor of two of the observations; this statistical metric is denoted fac2. In this work, we have chosen both the correlation (r) and fac2 to quantify model performance.

Model formulation under light winds

Several studies have been conducted for conditions with low wind speeds (e.g., Cimorelli et al., 2005; Carruthers et al., 1994). It was assumed that when the mean wind speed is below a certain threshold (0.1 m/s), the horizontal plume spread covers 360° (i.e., there is no well-defined wind direction). Venkatram et al. (2013) assumed that the vertical dispersion of the plume is linear with distance and derived the following formula for the contribution of the meandering components of the line source plume as:

$$C_{lw}(x,y,z) = \sqrt{\frac{2}{\pi}}\frac{qF(z)\theta_s}{2\pi u\sigma_z} \tag{3}$$

where θ_s is the angle subtended by the line source at the receptor.

$$\theta_s = \tan^{-1}\left(\frac{y_2 - y}{x}\right) + \tan^{-1}\left(\frac{y - y_1}{x}\right) \tag{4}$$

This concentration does not depend on wind direction.

Then, the concentration at a receptor is calculated as the sum of two terms, which represent the advected plume and the random spread of the meandering plume. A coefficient (f_r), which depends on wind speed, defines the relative importance of the advected plume and random spread components.

$$C = C_p(1 - f_r) + C_{lw}f_r \tag{5}$$

where $f_r = \frac{2\sigma_v^2}{u_e^2}$, and u_e is the effective velocity given by $u_e = \sqrt{(\sigma_u^2 + \sigma_v^2 + u^2)}$; $\sigma_v^2 = u^2\sinh(\sigma_\theta^2)$; and $\sigma_u^2 = u^2(\cosh(\sigma_\theta^2) - 1)$ are the standard deviations of the turbulent velocity fluctuations along the mean flow and in the lateral direction, respectively. σ_θ is the measured standard deviation of the horizontal wind direction fluctuations. We used by default σ_θ = 72° based on Cirillo and Poli (1992).

Field study

The traffic, meteorological, and air pollution data used in this study were obtained in the MOCoPo (Measuring and mOdelling traffic COngestion and POllution) project, which covered 4 periods (one in each season) during 2011 near freeway N87 located south of Grenoble in eastern France. Another project (PM-Drive; Particulate Matter, Direct and Indirect On-Road Vehicular Emissions) was conducted in part jointly with MOCoPo for a two-week campaign in September 2011, to obtain measurements of inorganic ions and trace metal concentrations every 4 h. The main objective of PM-Drive was to understand the chemical composition of PM from vehicle exhaust and non-exhaust emissions as well as their contributions to PM concentrations near roadways. Therefore, we focus here on the data from 11 till 27 September because the data set includes: (1) the classification of all vehicles circulating on freeway N87 according to vehicle categories, age and fuel used as well as pollutant emission regulation (vehicle fleet composition), (2) detailed traffic data relevant to traffic flow, including average vehicle speed and occupancy data (i.e. the fraction of time that the traffic count loop is occupied by a vehicle, a surrogate measurement of traffic density) every 6 min, and (3) air pollutant concentrations and meteorological data every 15 min, and (4) PM concentrations of inorganic ions and trace metal concentrations every 4 h. Most of these data are available at http://mocopo.ifsttar.fr.

Measurements of gaseous and PM species concentrations were conducted at two sites: the Echirolles site, which is the traffic site of this study and the Les Frenes site, which is the nearest urban background site for the Grenoble area from the local air quality network. The traffic site is located 7 m from the edge of the freeway, which is characterized by two lanes in each direction and a speed limit of 90 km/h. It carries over 68,000 vehicles daily with a peak hour count of 7800 vehicles/hour. The background site is located 1 km away from the freeway (Fig. 1).

The comparison of pollutant concentration measurements at the traffic and background sites determines the impacts due to the freeway traffic.

The near-road site is located 7 m from the roadway without any significant difference in elevation (see Fig. 2). It is, therefore, representative of maximum population exposure in the vicinity of traffic. Measurements of wind speed and direction (vane anemometer) and temperature were conducted on a 10 m mast. Air pollutant measurements were conducted at about 4 m agl. Nitrogen oxides (NO_x and NO, NO_2 by difference) were measured by chemiluminescence using a 15 min time step. PM_{10} and $PM_{2.5}$ were measured with TEOM instruments with a 15 min time step. In addition, PM_{10} was sampled

Fig. 1. Geographical location and characteristics of the Echirolles freeway including traffic (green dot), and background (red dot) sites. Source: Google Maps.

Fig. 2. View of the Echirolles (traffic) measurement site.

on quartz filters with a DA80 (30 m^3/h flow) with a 4 h time step for later chemical analysis of metals, ions, and carbonaceous compounds.

Traffic data

Given the traffic data and the input requirement of the steady-state atmospheric dispersion model, an emission model based on average vehicle speed was considered appropriate. Therefore, the CopCETE model (CETE Normandie Centre,

2010) of the French Ministry of Ecology was applied for exhaust and non-exhaust emissions. This model calculates vehicle emissions from most emission processes including vehicle exhaust, fuel evaporation, and equipment wear. It treats the road gradient, the length of the road segment, different types of traffic density (urban or rural road), fleet composition, including number of vehicles per categories (passenger, light-duty, and heavy-duty vehicles, buses) and their average speeds. This model uses emission functions from the European COPERT 4 methodology (Ntziachristos et al., 2009). CopCETE is based on the same methods and equations as COPERT 4, but with a mesoscopic approach that allows one to break down a road network into segments.

The traffic was measured with electromagnetic loops (SIREDO) on the segments of the freeway close to the traffic site, in both directions. The electromagnetic loops were used to estimate the average speed of the vehicles averaged over 6 min and total traffic count, regardless of vehicle types or lanes.

The road gradient and length of this freeway segment are 0% and 956 m, respectively. The fleet composition was obtained by image processing of vehicle front registration plates captured by four cameras located over the freeway as part of the MOCoPo project (in both directions). The identification of each vehicle was performed using data from the national registration file and allowed one to determine their detailed specifications (type of vehicle, year of registration, pollutant emission standard). Only 53% of the vehicles were identified because of experimental malfunctions and foreign registration plates.

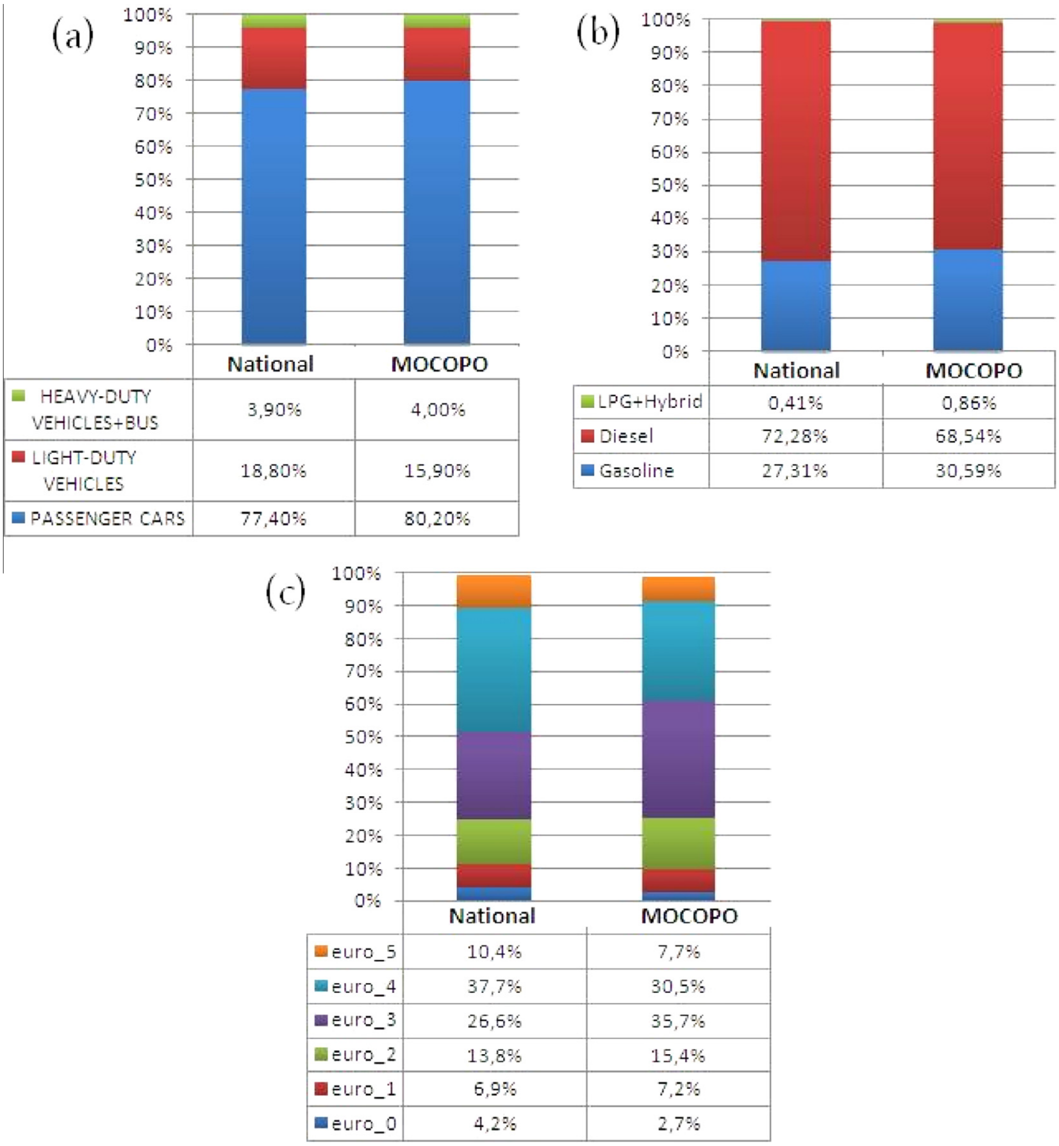

Fig. 3. Comparison of the national and local (MOCoPo) fleet compositions: (a) fuel category, (b) Euro standard category, (c) vehicle type category.

Nevertheless, this approach is considered to provide a reasonably accurate representation of the local fleet. The observed local fleet composition on freeway N87 (André et al., 2014) differs slightly from the national fleet composition of 2011 (André and Roche, 2013). Fig. 3 shows a comparison of the national and local (MOCoPo) fleet compositions presented by fuel categories for passenger cars, Euro standard (exhaust emission regulations, see Kousoulidou et al., 2008) for passenger cars, and vehicle categories. There are more passenger cars compared to the national fleet composition, and the fraction of diesel passenger cars is less than in the national fleet. The Euro 3 cars are the largest number of vehicles in the local data whereas the national fleet shows that Euro 4 cars dominate the fleet; therefore, the local data reflect an older fleet than the national data. The local fleet composition was used here.

Another parameter required by the CopCETE emission model is the average speed per vehicle category. The traffic data only include the vehicle mean speed and occupancy rates for all the vehicles. These data are used to estimate the state of congestion. The data depicting traffic flow as a function of occupancy rates are shown in Fig. 4 for both directions of the N87 freeway next to the traffic site. These data were used to determine the critical occupancy rate corresponding to the threshold of traffic congestion. The critical rate varies from 12% to 14% for both directions (see Fig. 4). Therefore, we considered that the traffic situations with an occupancy rate over 13% are congested and that the speed of passenger cars is considered equal to that of the heavy-duty vehicles above this threshold. For traffic situations that are not congested, the speed of passenger cars was taken to be 28 km/h greater than the speed of the heavy-duty vehicles (Hugrel and Joumard, 2004). As a sensitivity study, we calculated pollutant emissions with the assumption that the speed of passenger cars is equal to that of heavy-duty vehicles in all traffic situations. The results showed that the emissions of PM_{10} and NO_x increase only by 1% and 5%, respectively, in the latter case. The results presented below use the former case.

Emission data

The particulate matter (PM) emissions due to exhaust, tire, break, and clutch wear were calculated with the CopCETE model. Another important source of PM is re-emission of road dust by traffic. Dust resuspension by traffic depends on several factors such as vehicle speed, vehicle fleet composition, and time elapsed since the last rain event. Although algorithms exist to estimate dust resuspension based on such factors (e.g., Pay et al., 2011; Denby et al., 2013), there are still large uncertainties associated with such estimates. Therefore, a simple approach was used here that takes advantage of a statistical analysis of PM_{10} composition time series conducted by Polo Rehn at the traffic measurements site. Road dust contains particles originating from a wide range of sources. Polo Rehn and co-workers (Polo Rehn, 2013; Polo Rehn et al., 2014) used the PM-DRIVE data collected during the MOCoPo field campaign to estimate the contributions of emission source

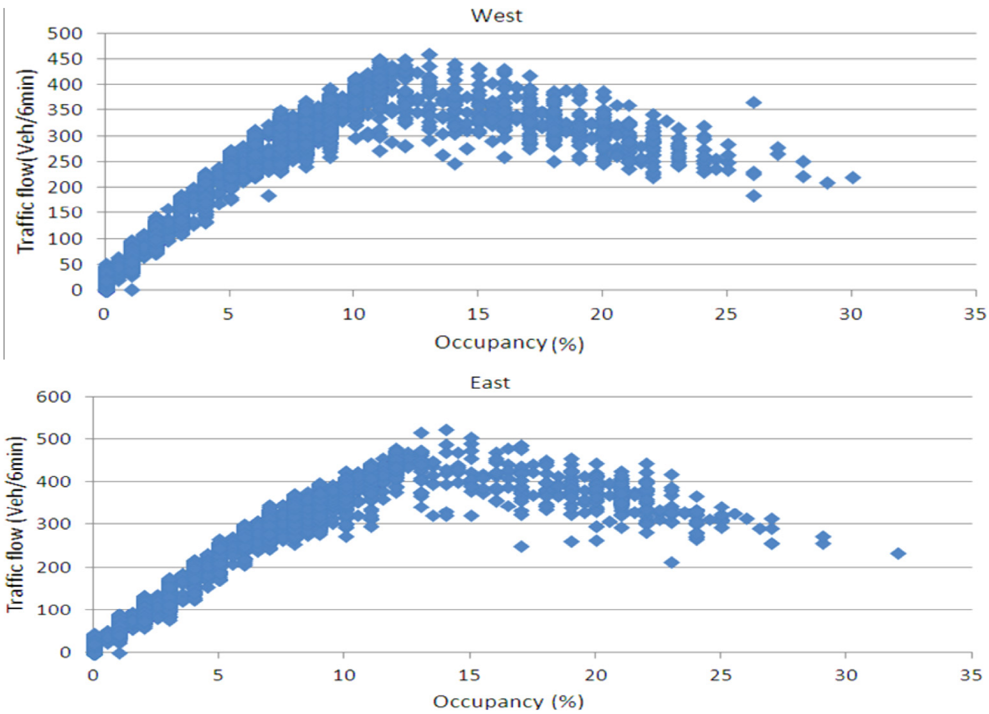

Fig. 4. Traffic flow (vehicles/6 min) versus occupancy data (%) in the east (bottom) and west (top) directions from the Echirolles measurement site. Occupancy can be seen as a surrogate measurement of traffic density (see text).

categories to PM concentrations measured at the traffic site using Positive Matrix Factorization (PMF). PMF is a principal component analysis method that can identify and quantify the relative contributions of various air pollution sources to ambient concentrations. It is a multivariate analysis based on determination of factors related to source profiles (Paatero and Tapper, 1994; Paatero, 1997). A data matrix (X) is decomposed into two matrices, a matrix of factors of contributions (G) and a matrix of factor profiles (F). In an air quality application, as was conducted by Polo Rehn (2013) at the traffic site in order to discriminate road dust resuspension, non-exhaust and exhaust traffic sources, X is a matrix which contains measured concentrations at distinct times of a series of chemical species (inorganic ions and trace metals), G is the matrix of the contributions of the source categories, and F is the matrix characterizing the chemical species profile of each source category. The equation is, therefore, written as follows:

$$X = FG + E \tag{6}$$

where E is the residual matrix (i.e., the unexplained part of X). It is the difference between the measured concentrations (X) and the concentrations modeled with PMF in the matrix $Y = FG$:

$$E = X - Y \tag{7}$$

The objective function to be minimized as a function of G and F is given by:

$$Q(E) = \sum_{i=1}^{m}\sum_{j=1}^{n}\left(\frac{e_{ij}}{\sigma_{ij}}\right)^2 \tag{8}$$

where σ_{ij} represents the uncertainty related to each concentration i and each measured species j. In this way, the PMF problem is then identified as a minimization of $Q(E)$ with respect to G and F, with the constraint that each element of the matrices G and F is to be non-negative.

PMF was applied to the PM-DRIVE data set to determine the contributions of major source categories to PM_{10} concentrations at the traffic site, including the contributions of PM_{10} resuspension and PM_{10} direct traffic emissions. The EPA PMF v3.0 was used. Polo Rehn and co-workers (Polo Rehn, 2013; Polo Rehn et al., 2014) showed that the contribution of PM_{10} resuspension represents on average over the period 76% of the emissions due to direct exhaust and tire, break, and clutch wear. Thus, a model simulation was conducted using a road dust resuspension emission term that was set to 76% of the vehicle emissions. However, dust resuspension was not taken into account during rain events (here on 19 September) since dust resuspension tends to be suppressed by rain. The hourly emissions of PM_{10} for cases with and without road dust resuspension are compared in Fig. 5.

The composition of road dust PM_{10} particles has been measured by Amato et al. (2011) for several metals, anions, and cations. Their study provides relative mean concentrations of major road dust components at three sites including Zurich, Switzerland, Barcelona and Girona, Spain. We used the average value among these three sites (Table 1) to estimate the emission rates of these species due to road dust resuspension. Therefore, the total emission rates of PM_{10} species are provided by the following equation:

$$q_{\text{species}} = q_{PM_{10}} \times f_{COPERT}(\text{species}) + q_{roaddust} \times f_{Amato}(\text{species}) \tag{9}$$

where the first term on the right hand side represents the direct vehicle emissions and the second term represents dust resuspension, q is the emission rate and f is the fraction of each species in PM_{10}. As discussed above, we assumed $q_{roaddust} = 0.76\ q_{PM10}$.

Finally, these data (as presented in Fig. 5) were used as input to the atmospheric dispersion model.

Meteorological data

The meteorological data included cloud cover, temperature, wind speed, and wind direction at the traffic site. Meteorological data were used here as hourly and 15 min averaged data. Fig. 6 shows that the measurement campaign took

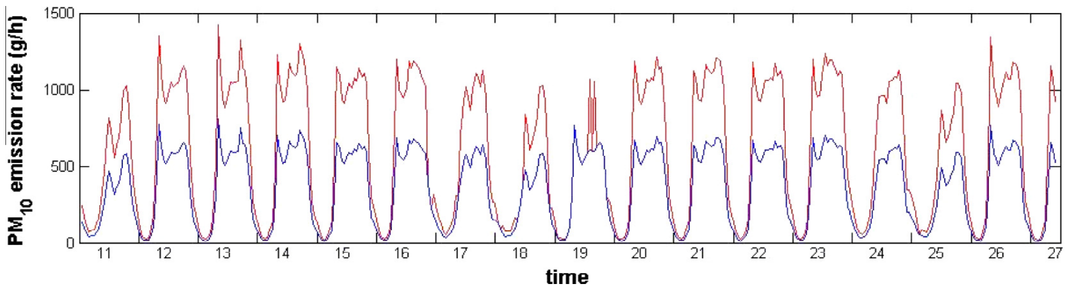

Fig. 5. Hourly emissions of the N87 freeway segment without resuspension (blue) and with resuspension (red) from 11 to 27 September 2011. (For interpretation of the references to colours in this figure legend, the reader is referred to the web version of this paper.)

Table 1
Relative mean concentrations of road dust components averaged over three urban sites (based on Amato et al., 2011) (μg g^{-1}).

Ca^{2+}	K^+	Na^+	NO_3^-	Fe	Mg^{2+}	Co	Cu	Mn	Pb	Sb	Sn
14×10^4	1.7×10^4	0.6×10^4	1.7×10^4	5.1×10^4	1.3×10^4	14.7	1978	580.3	207.7	194.7	243.3

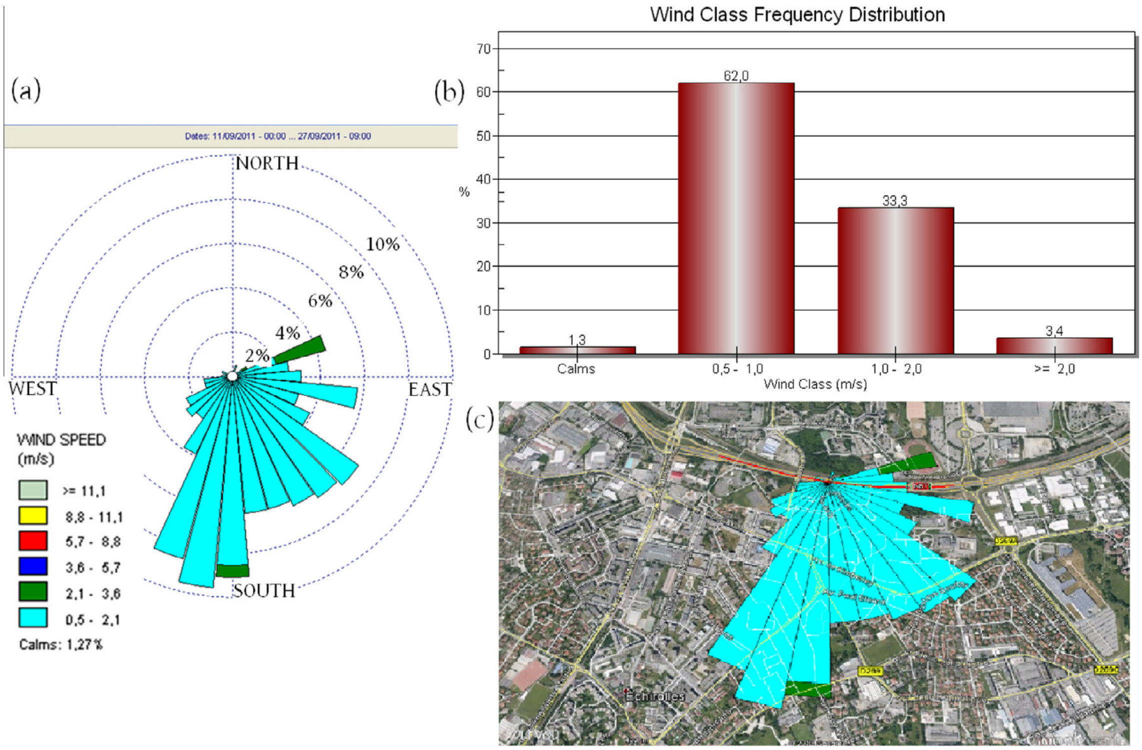

Fig. 6. Wind data at the traffic monitoring station: (a) wind rose, (b) wind speed frequency distribution, (c) configuration of the wind direction with respect to the N87 freeway segment.

place during a period characterized by low wind speeds. During 97% of the measurement period, the wind velocity was less than 2 m/s and it was less than 1 m/s more than 60% of the time. Furthermore, it appears that according to the wind directions, the measurement site is located mostly upwind of the freeway (about 90% of the time). Atmospheric stability was estimated following the Pasquill (1961) classification according to wind speed, day/night, and solar radiation (during the day) or cloudiness (at night).

Air quality data

Air quality data from 11 to 27 September 2011 are available for several air pollutants. The concentrations of NO, NO_2, PM_{10}, and $PM_{2.5}$ were measured at high frequencies and were subsequently aggregated as 1-h averaged values. Particulate species (trace metals and inorganic ions) were measured as 4-h averaged values from September 19 at 11:30 am till September 23 at 11:30 pm at the background site and from September 14 at 3:30 pm till September 23 at 11:30 pm at the traffic site. This 4-h temporal resolution was required for proper chemical analysis. It may not capture the full details of traffic flow, but it can distinguish among different traffic situations. These off-line measurements provided detailed chemical characterization of PM_{10}, which was used for instance to estimate the contribution of road dust resuspension (see above).

The PM_{10} analysis (Polo Rehn, 2013) was carried out by ICP-MS for a wide range of elements (Al, As, Ba, Ca, Cd, Ce, Co, Cr, Cs, Cu, Fe, K, La, Li, Mg, Mn, Mo, Na, Ni, Pb, Pd, Pt, Rb, Sb, Sc, Se, Sn, Sr, Ti, Tl, V, Zn, Zr). Only those metals that were detected at both sites were included in the analysis. The other pollutants measured include Cl^-, NO_3^-, SO_4^{2-}, $C_2O_4^{2-}$, Na^+, NH_4^+, K^+, Mg^{2+}, and Ca^{2+}. Ozone (O_3) was also measured at the background site and was used to account for NO_x/O_3 chemistry.

Results

The pollutants simulated in this study are NO_2, PM_{10}, $PM_{2.5}$, Na^+, NO_3^-, K^+, Mg^{2+}, Ca^{2+}, Co, Cu, Fe, Mn, Pb, Sb, and Sn based on data at both the background and traffic sites and emission factors availability. For example, emission factors for SO_4^{2-} and NH_4^+ were not available for road dust resuspension. The simulations were conducted with hourly input and output data and comparison with actual measurements was made for hourly and 4 h averages depending on data availability.

Chemical transformations leading to secondary particulate pollutants can be ignored here because of the close distance between the freeway and the measurement site, and particles were therefore assumed to be chemically inert. Thus, the concentrations of PM and particulate species at the traffic site were calculated as the sum of the background concentration measured at the background site and the traffic contribution obtained with Eqs. (5) and (9). For NO_2, the rapid reactions between NO, NO_2 and O_3 were taken into account. The Leighton steady-state relationship was used to calculate the NO_2 concentrations from the NO_x concentration at the traffic site and the concentrations of NO, NO_2 and O_3 at the background site (e.g., Briant et al., 2013). We considered a fraction of 26% of NO_2 and 74% of NO for NO_x traffic emissions based on the fleet composition of the N87 freeway and the COPERT 4 data.

Two simulations were conducted: one with the standard Gaussian plume model (Eq. (1)) referred to as the standard model, and one with the Gaussian plume model modified with the option to account for conditions with light winds (Eq. (5)). They are compared here to evaluate the effect of the light wind algorithm. They were performed for PM_{10}, $PM_{2.5}$, a selection of PM_{10} chemical species, and NO_2.

Fig. 7 shows simulated and measured concentrations of PM_{10}. The simulation follows the temporal evolution of the measurements; however, some observed peaks are not reproduced by the simulation (for example on 12, 21, and 27 September at 9 am, and 26 September at 8 am).

The performance of the two models is presented in Table 2 in terms of statistical results, which include the Root Mean Square Error (RMSE), the Mean Normalized Error (MNE), the Mean Normalized Bias (MNB), the Normalized Mean Error (NME), and the Mean Fractional Error (MFE) (see Yu et al., 2006, for definition of the metrics). The model underestimates the concentrations of PM_{10} and $PM_{2.5}$. For PM_{10}, the correlation between measured and simulated values is satisfactory ($r = 0.76$; $n = 394$) and, therefore explains more than half of the observed variability ($r^2 > 0.5$). Similar results are obtained for $PM_{2.5}$. When comparing the results of the modified model with those from the standard model (see Fig. 8), which neglects the impacts of light winds under calm conditions, it appears that the treatment of calm conditions leads to a significant improvement in the correlation of PM_{10} from 0.48 to 0.76. Similar results are obtained for $PM_{2.5}$ with an improvement from 0.41 to 0.72 in the correlation coefficient. The comparison of the two models for PM_{10} shows that RMSE, MNE, MNB, NME, and MFE decrease by 40%, 29%, 0%, 28%, and 27%, respectively when adding the option for calm winds. The corresponding decreases for $PM_{2.5}$ are 40%, 32%, 8%, 30%, and 26%. These significant decreases of the errors for the modified model highlight the importance of the calm wind algorithm to better simulate pollutant concentrations under such conditions.

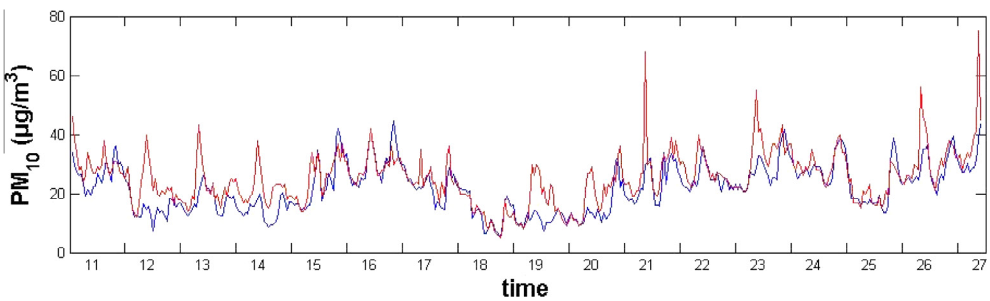

Fig. 7. Comparison of PM_{10} hourly concentrations measured (red) and simulated with the calm option (blue) at the traffic site. (For interpretation of the references to colours in this figure legend, the reader is referred to the web version of this paper.)

Table 2
Statistical performance for NO_2, PM_{10}, and $PM_{2.5}$ concentrations for the standard model (Eq. (1)) and the model modified for calm conditions (Eq. (5)).

	Number of samples	Average measured value (μg m^{-3})	Average modeled value (μg m^{-3})	Correlation coefficient	RMSE (μg m^{-3})	MNE	MNB	NME	MFE
PM_{10} (Eq. (5))	394	25.2	21.9	0.76	6.8	0.17	−0.12	0.18	0.19
PM_{10} (Eq. (1))			21.4	0.48	11.2	0.24	−0.12	0.25	0.26
$PM_{2.5}$ (Eq. (5))	394	19.9	17.1	0.72	5.6	0.17	−0.11	0.19	0.2
$PM_{2.5}$ (Eq. (1))			16.6	0.41	9.4	0.25	−0.13	0.27	0.27
NO_2 (Eq. (5))	355	51.2	31.8	0.44	28.4	0.4	−0.35	0.43	0.56
NO_2 (Eq. (1))			27	0.23	34.3	0.52	−0.4	0.55	0.72

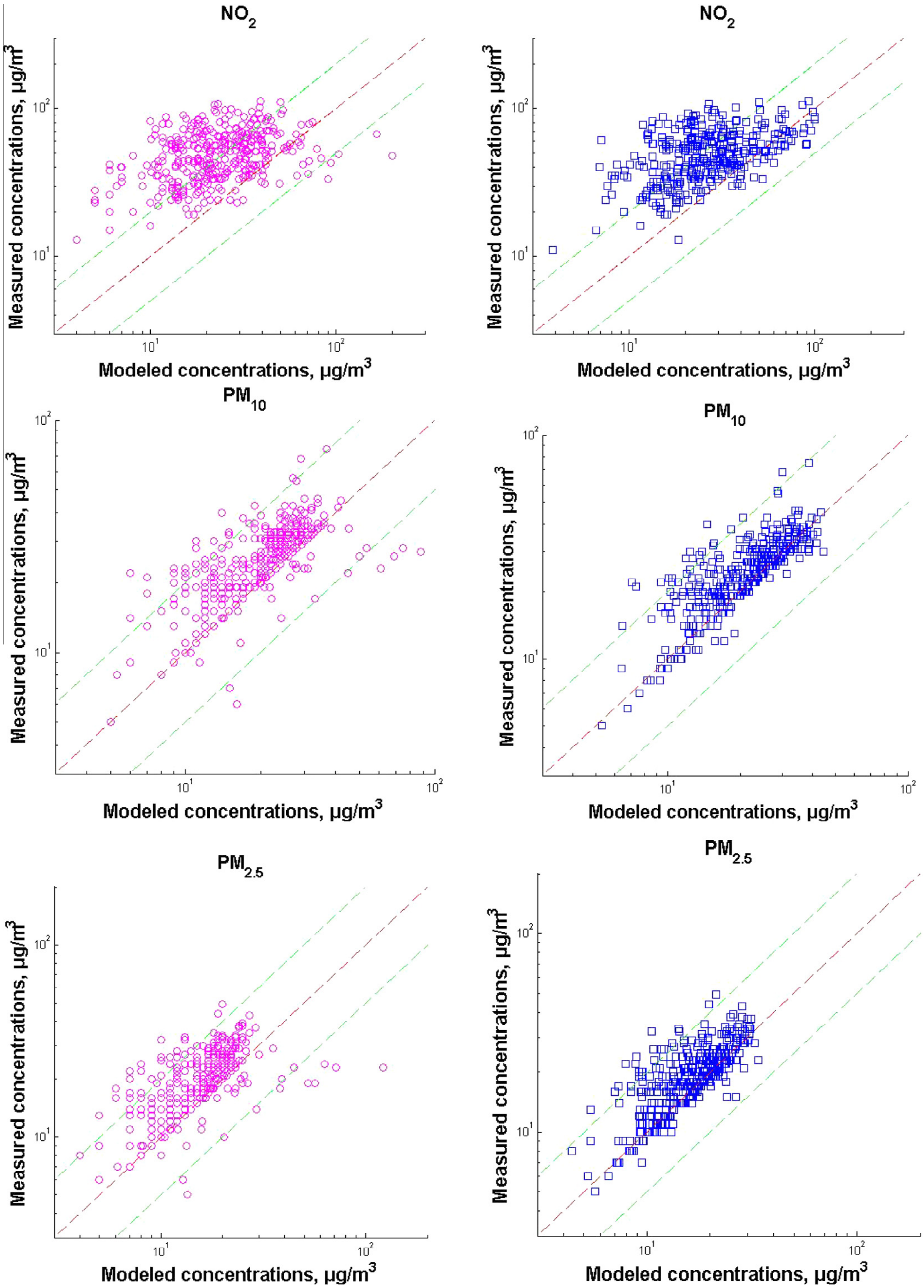

Fig. 8. Comparison of concentrations of the standard model (pink, left side) and the model modified for calm conditions (blue, right side) with measured concentrations of NO_2, PM_{10}, and $PM_{2.5}$. (For interpretation of the references to colours in this figure legend, the reader is referred to the web version of this paper.)

It is of interest to investigate whether the location of the measurement site with respect to the road, downwind or upwind, has a significant effect on model performance and/or the effect of the incorporation of the light wind parameterization (i.e., Eq. (5) vs Eq. (1)). The same performance statistics are, therefore, presented in Table 3 for the two subsets of the sampling data corresponding to the location of the measurement site with respect to the road (i.e., downwind subset and upwind subset). The statistics show better model performance for PM_{10} and $PM_{2.5}$ with the modified model (Eq. (5)) compared to the standard model (Eq. (1)) whether the measurement site is upwind or downwind of the road.

For the cases where the site is downwind of the road, the improvement in model performance is due in part to the overestimation of the PM concentrations by the standard model; incorporating the light wind parameterization lowers the modeled concentrations since the emissions are then dispersed in all directions rather than only downwind. If the standard model had underestimated the measured concentrations, model performance would have deteriorated in terms of bias and error. This appears for the downwind NO_2 concentrations for which the model overestimation is less than that for PM (ratio of the average modeled and measured values of 1.23 for NO_2, compared to 1.44 for PM_{10} and 1.49 for $PM_{2.5}$) and the performance of the modified model is better than that of the standard model only for correlation and RMSE.

For the cases where the site is upwind of the road (about 90% of the cases), the improvement in model performance due to the parameterization of light wind conditions is expected since the standard model consistently underestimates and, consequently, model performance improves for all three pollutants and all statistics. One notes that although the decrease in model error and bias is significant in all cases, the improvement in the correlation is slight for the upwind cases.

Wind speeds were low during this study with a wind speed less than 1.5 m/s 84% of the time and less than 1 m/s more than 60% of the time. Therefore, no clear trend appears in terms of model performance as a function of wind speed (using thresholds of 1 and 1.5 m/s); the standard model overestimates at all wind speeds when the measurement site is downwind of the road and underestimates at all wind speeds when it is upwind. Correlation between modeled and measured concentrations improves with the modified model at all wind speeds, except for NO_2, where a decrease in the correlation coefficient from about 0.5 to 0.25 occurs for wind speeds above 1 m/s when the site is upwind of the road. Nevertheless, a slight improvement in correlation from 0.41 to 0.44 occurs when all upwind cases are considered.

The categorization of model performance as a function of atmospheric stability was investigated for correlation between measured and modeled concentrations using three main categories in order to have sufficient cases in each category: unstable conditions (classes A and B), slightly unstable and neutral conditions (classes C and D) and stable conditions (classes E and F). The standard model showed for the three pollutants (i.e., PM_{10}, $PM_{2.5}$, and NO_2) better correlations (about 0.8 or greater) for slightly unstable and neutral conditions and worse correlations (less than 0.4) for unstable conditions. The modified model does not show such clear trends although better correlations are obtained either for slightly unstable and neutral conditions or for stable conditions.

The performance of both models is poorer for the simulation of NO_2 concentrations. Both models significantly underestimate the NO_2 concentrations overall with a correlation of 0.44 and a mean normalized error of 40–50%. Although performance is poorer than those obtained for PM_{10} and $PM_{2.5}$, the modified model still improves this performance.

The PM_{10}, $PM_{2.5}$, and NO_2 concentrations were also simulated at a fine temporal resolution (15 min) using the modified model. The average concentrations are similar to those of the 1 h simulation for PM_{10} and $PM_{2.5}$ but the average NO_2 concentration decreases to 21.2 $\mu g\, m^{-3}$ with this finer time resolution. The correlation coefficients for PM_{10}, $PM_{2.5}$, and NO_2 decrease to 0.71, 0.66, and 0.39, respectively. Therefore, a finer temporal resolution does not improve model performance as it becomes increasingly difficult to match the time series of the observed concentrations.

Table 3
Statistical performance for NO_2, PM_{10}, and $PM_{2.5}$ concentrations for the standard model (Eq. (1)) and the model modified for calm conditions (Eq. (5)) as a function of wind direction: measurement site located downwind of the road (top) and upwind of the road (bottom).

	Number of samples	Average measured value ($\mu g\ m^{-3}$)	Average modeled value ($\mu g\ m^{-3}$)	Correlation coefficient	RMSE ($\mu g\ m^{-3}$)	MNE	MNB	NME	MFE
Downwind of the road									
PM_{10} (Eq. (5))	42	21.7	17.4	0.74	6.6	0.18	−0.16	0.21	0.22
PM_{10} (Eq. (1))			31.2	0.43	24.7	0.58	0.44	0.59	0.37
$PM_{2.5}$ (Eq. (5))	42	17.3	14.3	0.70	5.4	0.19	−0.14	0.21	0.23
$PM_{2.5}$ (Eq. (1))			25.8	0.46	20.7	0.59	0.48	0.61	0.37
NO_2 (Eq. (5))	37	45.1	20.8	0.38	29.2	0.50	−0.50	0.54	0.72
NO_2 (Eq. (1))			55.6	0.27	38.5	0.51	0.27	0.53	0.39
Upwind of the road									
PM_{10} (Eq. (5))	352	25.6	22.2	0.77	6.8	0.16	−0.12	0.17	0.19
PM_{10} (Eq. (1))			20.2	0.73	8.2	0.20	−0.20	0.22	0.25
$PM_{2.5}$ (Eq. (5))	352	20.3	17.4	0.72	5.7	0.17	−0.12	0.19	0.20
$PM_{2.5}$ (Eq. (1))			15.6	0.68	7.0	0.21	−0.20	0.24	0.26
NO_2 (Eq. (5))	318	51.9	33.0	0.43	28.3	0.39	−0.34	0.42	0.54
NO_2 (Eq. (1))			23.7	0.41	33.8	0.52	−0.52	0.55	0.76

NO_2 concentrations near a freeway are strongly influenced by local NO_x traffic emissions because of the rapid chemical transformations of NO to NO_2, while the contribution of the background air is less important than it is for PM concentrations. Therefore, the results obtained for NO_2 are more representative of model performance than the results for PM_{10} and $PM_{2.5}$, which depend more strongly on background pollution. Our results indicate that pollutant dispersion near a roadway under calm conditions is difficult to simulate, although the option for light wind conditions improves performance significantly (for example, the correlation coefficient nearly doubles). However, it appears necessary to further improve the model formulation for these conditions.

Fig. 9 illustrates for 15 species the ratio of the average concentration for the whole period near the freeway at the traffic site and the same concentration at the background site. The ratios are presented for the measured and simulated concentrations. The pollutants are presented from left to right in terms of decreasing measured ratio, i.e., the species concentrations impacted most by traffic are to the left.

The measured and modeled concentrations of anions, cations, and metals averaged over the measurement period at the traffic site are presented in Table 4 along with the modified model performance statistics. Scatter plots are presented in Fig. 10 for each pollutant. Cu and Sb show the greatest impact of traffic emissions and the lowest correlation (<11%) between measurement and simulation. The model overestimates the measured value, which may be due to inappropriate emission factors. Other pollutants that are overestimated are Mg^{2+} and Pb. Their non-exhaust emission factors are based on data obtained between 1983 and 2007. They are likely to overestimate current Pb emissions because of reductions in Pb non-exhaust emissions in recent years. For example, Hjortenkrans et al. (2007) showed that Pb emissions from brake linings in Stockholm, Sweden, were reduced from 560 kg/year in 1993 to 35 kg/year in 2005. Except for Co, the other pollutants show satisfactory correlation coefficients (greater than 69%) with the modified model. However, model performance is more meaningful for those species that include a significant traffic contribution (see Fig. 9). The emission factors of Amato et al. (2011) were used here as generic emission factors. Better results would be obtained if the site-specific emission profile obtained by Polo Rehn (2013) for road dust were used, since that profile was derived from the traffic site measurements; however, such a model performance evaluation would be less meaningful because it would use as input the same emission

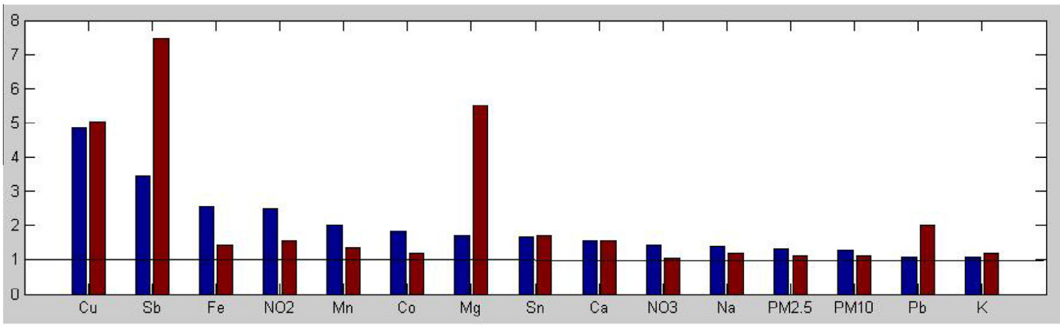

Fig. 9. Ratio of the concentrations at the traffic and background sites: measured values (blue, left side) and modeled values (red, right side). (For interpretation of the references to colours in this figure legend, the reader is referred to the web version of this paper.)

Table 4
Statistical performance for inorganic ions and trace metals for the model modified for calm conditions. The correlation is also presented for the standard model.

Statistical criterion	Pollutants											
	Ca^{2+}	K^+	Na^+	NO_3^-	Mg^{2+}	Co	Cu	Fe	Mn	Pb	Sb	Sn
Number of samples	48	48	48	48	48	28	25	28	27	28	28	28
Average measured value ($\mu g\ m^{-3}$)	420	74	85	565	17	0.26	49.6	1371	15.6	5.9	4.75	15.2
Average estimated value ($\mu g\ m^{-3}$)	378	81.9	73.4	409	55.3	0.17	51.3	765	10.5	11.1	10.3	15.5
Correlation	0.78	0.84	0.69	0.8	0.05	0.57	0.11	0.93	0.82	0.36	0.1	0.97
(*P*-value)	(0)	(0)	(0)	(0)	(0.37)	(0)	(0.3)	(0)	(0)	(0.03)	(0.31)	(0)
(Eq. (5))												
Correlation	0.52	0.55	0.29	0.78	0.01	0.2	0.3	0.51	0.67	0.11	−0.3	0.68
(*P*-value)	(0)	(0)	(0.02)	(0)	(0.47)	(0.15)	(0.07)	(0)	(0)	(0.29)	(0.06)	(0)
(Eq. (1))												
RMSE ($\mu g\ m^{-3}$)	167	19.7	34.3	235	64	0.1	49.5	881	8.7	7.8	10.5	6.34
MNE	0.44	0.2	0.22	0.26	2.58	0.38	0.87	0.4	0.4	1.25	1.75	0.55
MNB	−0.02	0.12	−0.1	−0.2	2.56	−0.3	0.43	−0.4	−0.3	1.24	1.57	0.19
NME	0.33	0.18	0.24	0.29	2.29	0.39	0.7	0.45	0.39	0.9	1.41	0.31
MFE	0.45	0.17	0.24	0.33	0.78	0.53	0.65	0.57	0.5	0.58	0.72	0.49

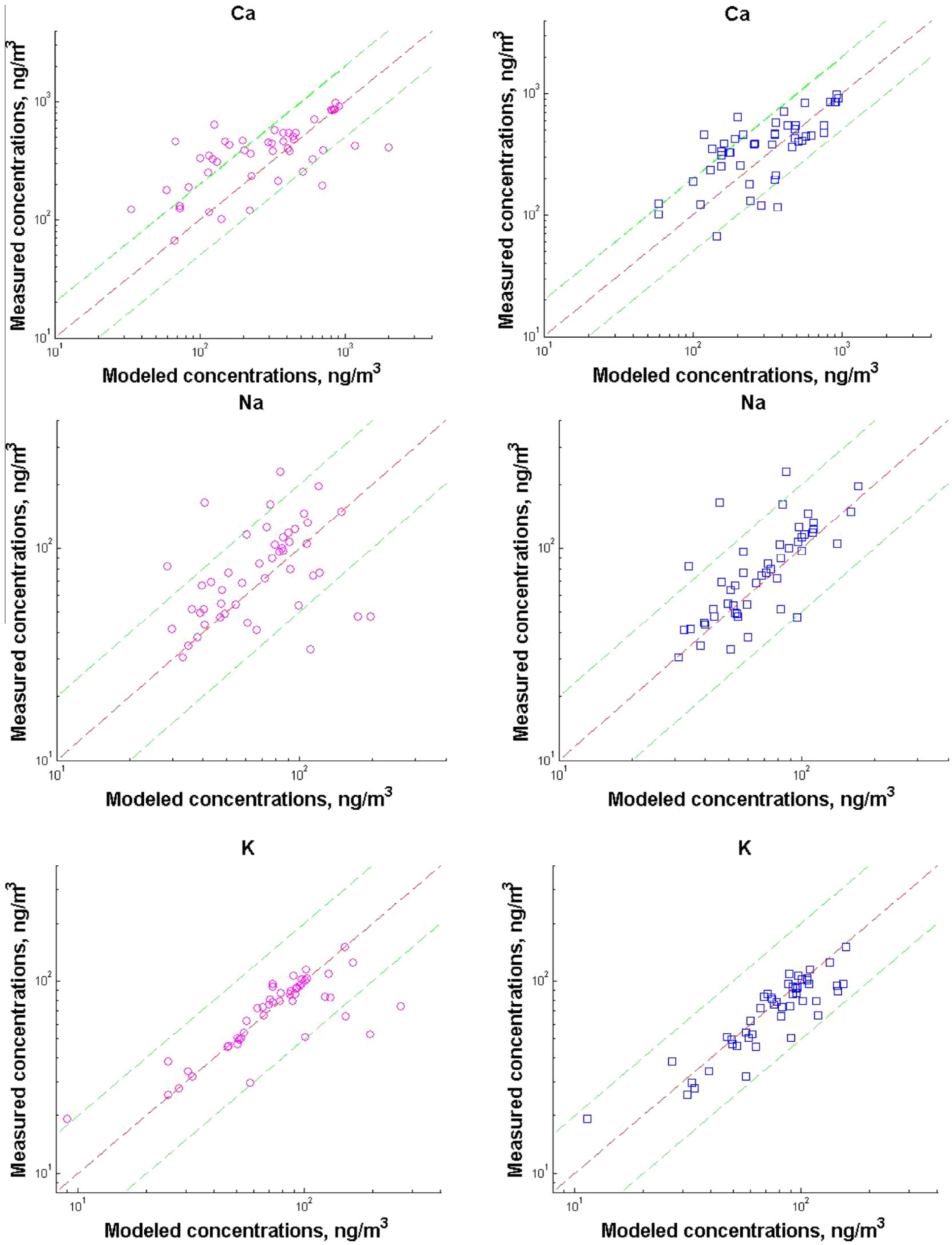

Fig. 10. Comparison of concentrations modeled with the standard model (pink circles, left side) and with the modified model (blue squares, right side) with measured concentrations at the traffic site for inorganic ions and trace metals. (For interpretation of the references to colours in this figure legend, the reader is referred to the web version of this paper.)

profile as seen in the observations. Better correlations are obtained with the model that considers calm conditions than with the standard model.

According to Chang and Hanna (2004), a "good" model would be expected to have about 50% of the predictions within a factor of two (fac2) of the observations, a relative mean bias (RMB) within ±30%, and a relative scatter (RS) of about a factor of two or three. These values, which are provided in Table 5, confirm that the "modified model" can be considered as a "good"

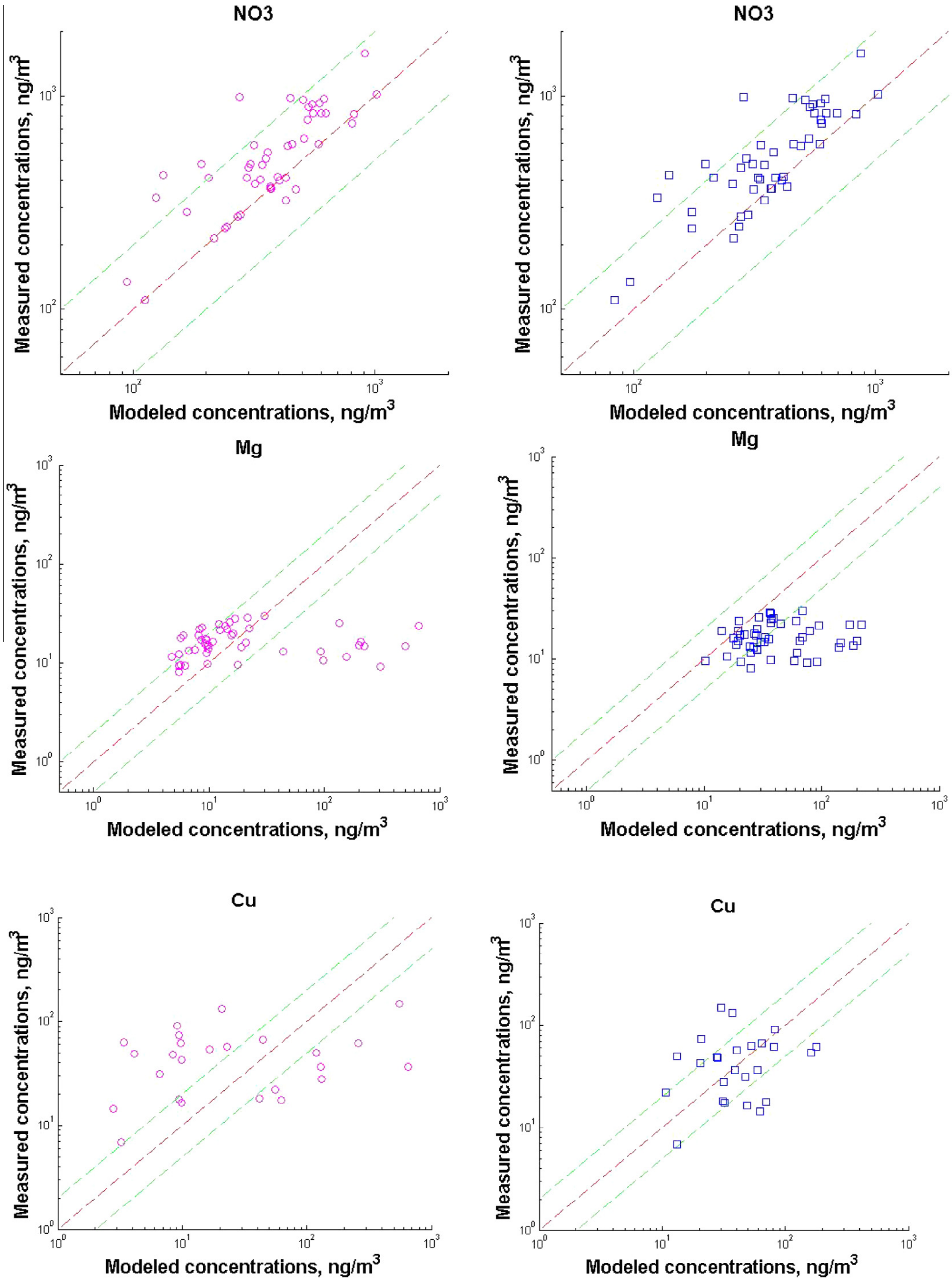

Fig. 10 (*continued*)

model for predictions of PM_{10}, $PM_{2.5}$, Na^+, NO_3^-, K^+, Ca^{2+}, Cu, and Sn concentrations. However, these criteria are not met for predictions of NO_2, Mg^{2+}, Co, Fe, Mn, Pb, and Sb.

The consideration of vehicle turbulence effects during stable atmospheric conditions may improve the model. Several studies have proposed modifications of the vertical dispersion coefficient as a function of vehicle-induced turbulence (VIT) (Eskridge and Rao, 1986; Kastner-Klein et al., 2000; Di Sabatino et al., 2003; Bäumer et al., 2005). An empirical model

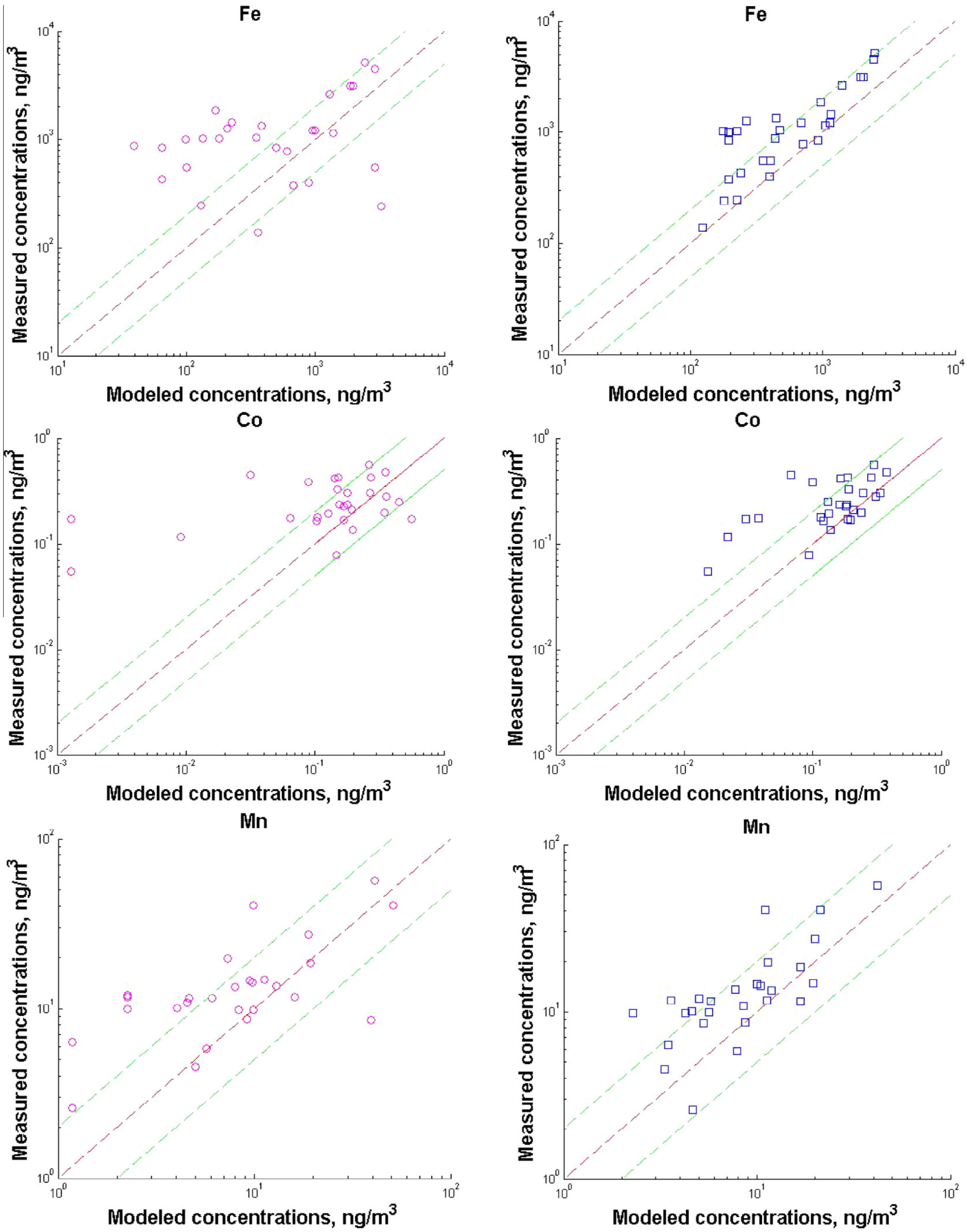

Fig. 10 (*continued*)

(Kastner-Klein et al., 2000) was applied here to account for the effects of VIT based on the hourly velocity, density, frontal area and drag coefficients of the vehicles. This formulation did not lead to significant effect of VIT on pollutant dispersion and, therefore, on model performance. Parameterizations of VIT mostly affect the vertical dispersion of the air pollutants, but do not reflect the possible impact on horizontal transport under calm conditions. Further work appears warranted to improve VIT parameterizations under such challenging conditions. CFD modeling (e.g., Wang and Zhang, 2009) may provide useful insights in that regard.

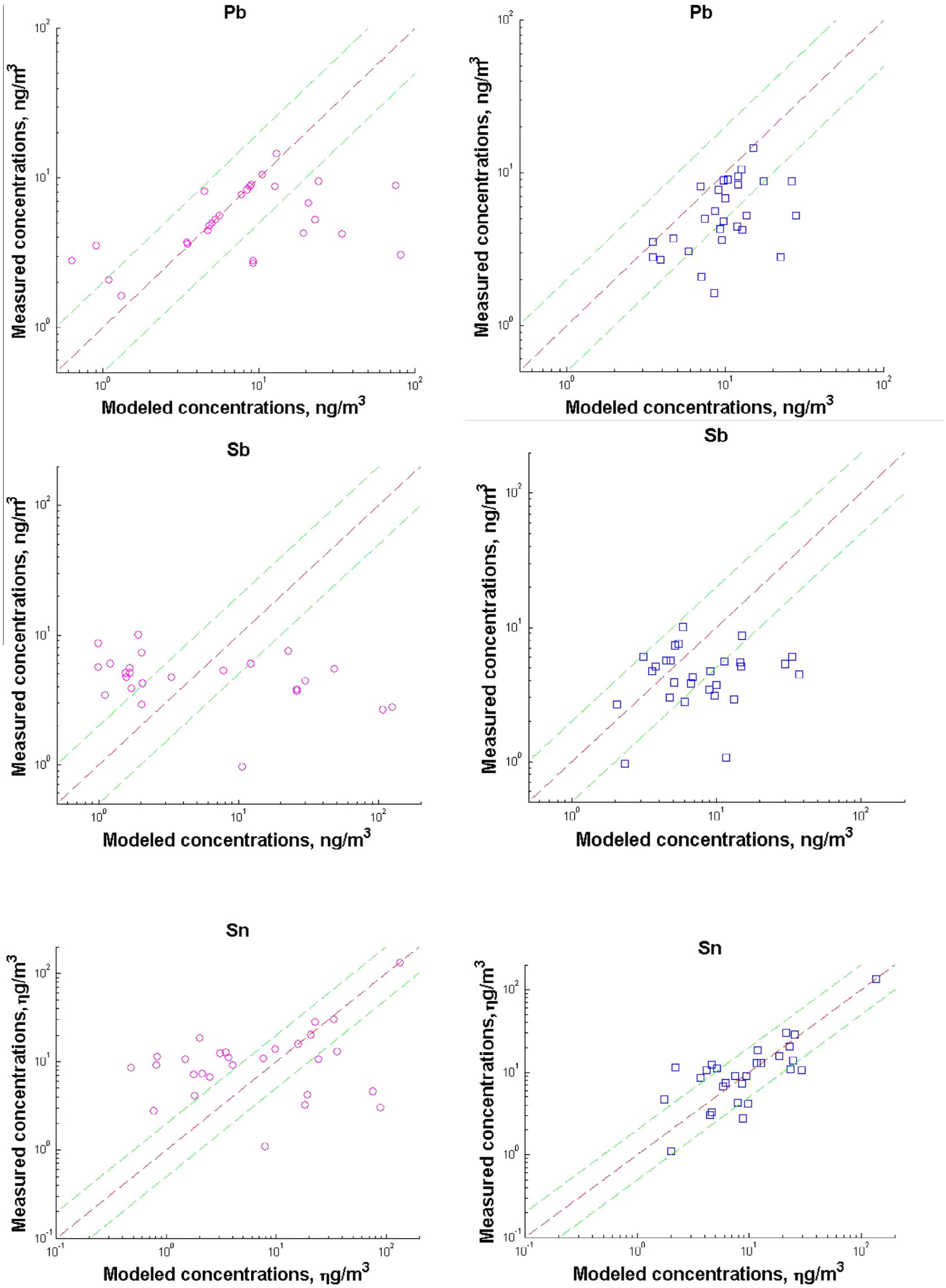

Fig. 10 (*continued*)

Table 5
Performance indicators of the model modified for calm conditions.

	PM_{10}	$PM_{2.5}$	NO_2	Ca^{2+}	K^+	Na^+	NO_3^-	Mg^{2+}	Co	Cu	Fe	Mn	Pb	Sb	Sn
RMB	−0.14	−0.15	−0.61	−0.1	0.1	−0.15	−0.32	1.06	−0.4	0.03	−0.6	−0.39	0.61	0.74	0.02
RS	0.85	0.85	0.48	0.84	1.1	0.89	0.73	2.53	0.58	1.02	0.53	0.66	1.88	1.82	0.97
fac2	0.95	0.94	0.45	0.75	1	0.92	0.9	0.42	0.71	0.56	0.68	0.74	0.57	0.54	0.64

Conclusion

In this study, we estimated the atmospheric dispersion of pollutant emitted by vehicles near a freeway under calm meteorological situations. To that end, an average-speed emission model was applied to estimate vehicle emissions with local traffic data. In addition, PM resuspension by traffic was included based on results of a site-specific PMF analysis. The concentrations of NO_2, PM_{10}, $PM_{2.5}$, Na^+, NO_3^-, K^+, Mg^{2+}, Ca^{2+}, Co, Cu, Fe, Mn, Pb, Sb and Sn were simulated and compared with observations at a receptor site located 7 m from the freeway. The standard Gaussian plume model was modified to account for calm conditions. In this modified formulation, the plume of pollutants from the freeway includes two terms: a classic Gaussian plume, which extends from the freeway downstream in the direction of the wind, and a plume extending in all directions close to the road. The results of the modified and standard models were compared to measurements and showed that the treatment of calm conditions improves the correlation coefficient significantly and reduces the errors. However, it appears necessary to further develop this formulation, a possible way being to better represent the effect of VIT on the horizontal transport of pollutants under such calm conditions. Another area for improvement is a better characterization of the various emission factors, for both direct and indirect (dust resuspension) sources.

Acknowledgments

The authors thank the "Ville numérique" program; IFSTTAR; CEREA, a joint laboratory of École des Ponts ParisTech and EDF R&D; the MOCoPo project funded by PREDIT; and the PM-DRIVE project funded by the CORTEA program of ADEME (program n° 1162C0002) for their financial support.

References

Amato, F., Pandolfi, M., Moreno, T., Furger, M., Pey, J., Alastuey, A., Bukowiecki, N., Prevot, A.S.H., Baltensperger, U., Querol, X., 2011. Sources and variability of inhalable road dust particles in three European cities. Atmos. Environ. 45, 6777–6787.

André, M., Roche, A.L., Bourcier, L. 2013. Statistiques de parcs et trafic pour le calcul des émissions de polluants des transports routiers pour la France. In French. Rapport IFSTTAR LTE, Bron (France), 132pp.

André, M., Chanut, H., Pasquier, A., Pellet, C., Montenon, A., 2014. Modélisation et estimation des émissions de polluants du trafic routier. Rapport 7.1, Projet MOCoPo (Mesure et mOdélisation de la COngestion et de la Pollution), In French, Contrat n° 2010 MT CVS 121.

Baldauf, R., Thoma, E., Hays, M., Shores, R., Kinsey, J., Gullett, B., Kimbrough, S., Isakov, V., Long, T., Snow, R., Khlystov, A., Weinstein, J., Chen, F.L., Seila, R., Olson, D., Gilmour, I., Cho, S.H., Watkins, N., Rowley, P., Bang, J., 2008. Traffic and meteorological impacts on near-road air quality: summary of methods and trends from the Raleigh Near-Road Study. J. Air Waste. Manag. Assoc. 58 (7), 865–878.

Bäumer, D., Vogel, B., Fiedler, F., 2005. A new parameterisation of motorway-induced turbulence and its application in a numerical model. Atmos. Environ. 39 (31), 5750–5759.

Benson, P.E., 1989. CALINE4 – A Dispersion Model for Predicting Air Pollution Concentration Near Roadways. Office of transportation laboratory, California department of transportation, Sacramento, CA.

Briant, R., Korsakissok, I., Seigneur, C., 2011. An improved line source model for air pollutant dispersion from roadway traffic. Atmos. Environ. 45, 4099–4107.

Briant, R., Seigneur, C., Gadrat, M., Bugajny, C., 2013. Evaluation of roadway Gaussian plume models with large-scale measurement campaigns. Geoscientific Model Dev. 6, 445–446.

Briggs, G. (1973). Diffusion estimation for small emissions. Report NOAA n. 79, Oak Ridge, TN (U.S.A.).

Carruthers, D., Holroyd, R., Hunt, J., Weng, W., Robins, A., Apsley, D., Thompson, D., Smith, F., 1994. UK-ADMS: a new approach to modeling dispersion in the earth's atmospheric boundary layer. J. Wind Eng. Ind. Aerodynamics 52, 139–153.

CETE Normandie Centre and DADT Département aménagement durable des territoires, 2010. User guide of COPCETE v3.

Chang, J., Hanna, S., 2004. Air quality model performance evaluation. Meteorol. Atmos. Phys. 87, 167–196.

Cimorelli, A.J., Perry, S.G., Venkatram, A., Weil, J.C., Paine, R.J., Wilson, R.B., Lee, R.F., Peters, W.D., Brode, R.W., 2005. AERMOD: a dispersion model for industrial source applications. Part I: general model formulation and boundary layer characterization. Appl. Meteorol. 44, 682–693.

Cirillo, M.C., Poli, A.A., 1992. An intercomparison of semi-empirical diffusion models under low wind speed, stable conditions. Atmos. Environ., Part A 26, 765–774.

Denby, B.R., Sundvor, I., Johansson, C., Pirjola, L., Ketzel, M., Norman, M., Kupiainen, K., Gustafsson, M., Blomqvist, G., Omstedt, G., 2013. A coupled road dust and surface moisture model to predict non-exhaust road traffic induced particle emissions (NORTRIP). Part 1: Road dust loading and suspension modeling. Atmos. Environ. 77, 283–300.

Di Sabatino, S., Kastner-Klein, P., Berkowicz, R., Britter, R.E., Fedorovich, E., 2003. The modelling of turbulence from traffic in urban dispersion models. Part I: theoretical considerations. Environ. Fluid Mech. 3 (2), 129–143.

Eskridge, R., Rao, S., 1986. Turbulent diffusion behind vehicles: experimentally determined turbulence mixing parameters. Atmos. Environ. 20 (5), 851–860.

Garshick, E., Laden, F., Hart, J.E., Caron, A., 2003. Residence near a major road and respiratory symptoms in U.S. Veterans. Epidemiology 14, 728–736.

Gauderman, W.J., Avol, E., Lurmann, F., Kuenzli, N., Gilliland, F., Peters, J., McConnell, R., 2005. Childhood asthma and exposure to traffic and nitrogen dioxide. Epidemiology 16, 737–743.

Heinrich, J., Topp, R., Gehring, U., Thefeld, W., 2005. Traffic at residential address, respiratory health, and atopy in adults: the national german health survey 1998. Environ. Res. 98, 240–249.

Hirtl, M., Baumann-Stanzer, K., 2007. Evaluation of two dispersion models (ADMS-Roads and LASAT) applied to street canyons in Stockholm, London and Berlin. Atmos. Environ. 41, 5959–5971.

Hjortenkrans, D.S., Bergbäck, B.G., Häggerud, A.V., 2007. Metal emissions from brake linings and tires: case studies of Stockholm, Sweden 1995/1998 and 2005. Environ. Sci. Technol. 41, 5224–5230.

Holmes, N.S., Morawska, L., 2006. A review of dispersion modelling and its application to the dispersion of particles: an overview of different dispersion models available. Atmos. Environ. 40, 5902–5928.

Hugrel, C. and Joumard, R. (2004). French fleet composition (1970–2025). Rapport LTE N° 0420.2004, IFSTTAR, Bron, France.

Janssen, N.A.H., van Vliet, P.H.N., Aarts, F., Harssema, H., Brunekreef, B., 2002. Assessment of exposure to traffic related air pollution of children attending schools near motorways. Atmos. Environ. 35, 3875–3884.

Kastner-Klein, P., Berkowicz, R., Plate, E.J., 2000. Modelling of vehicle-induced turbulence in air pollution studies for streets. Int. J. Environ. Pollut. 14, 496–507.

Kenty, K.L., Poor, N.D., Kronmiller, K.G., McClenny, W., King, C., Atkeson, T., Campbell, S.W., 2007. Application of CALINE4 to roadside NO/NO_2 transformations. Atmos. Environ. 41, 4270–4280.
Kousoulidou, M., Ntziachristos, L., Mellios, G., Samaras, Z., 2008. Road-transport emission projections to 2020 in European urban environments. Atmos. Environ. 42, 7465–7475.
McConnell, R., Berhane, K., Yao, L., Jerrett, M., Lurmann, F., Gilliland, F., Kuenzli, N., Gauderman, J., Avol, E., Thomas, D., Peters, J., 2006. Traffic, susceptibility, and childhood asthma. Environ. Health Perspect. 114, 766–772.
Misra, A., Roorda, M.G., MacLean, H.L., 2013. An integrated modelling approach to estimate urban traffic emissions. Atmos. Environ. 73, 81–91.
Ntziachristos, L., Gkatzoflias, D., Kouridis, C., Samaras, Z., 2009. COPERT: a European road transport emission inventory model. In Information Technologies in Environmental Engineering. In: Athanassialis, I.N. et al. (Eds.), Environmental Science and Engineering. Springer-Verlag, Berlin Heidelberg, pp. 491–504.
Paatero, P., 1997. Least squares formulation of robust non-negative factor analysis. Chemom. Intell. Lab. Syst. 37, 23–35.
Paatero, P., Tapper, U., 1994. Positive matrix factorization: a non-negative factor model with optimal utilization of error estimates of data values. Environmetrics 5, 111–126.
Pasquill, F., 1961. Atmospheric dispersion modeling. Meteorol. Mag. 90, 33–49.
Pay, M.T., Jiménez-Guerrero, P., Baldasano, J.M., 2011. Implementation of resuspension from paved roads for the improvement of CALIOPE air quality system in Spain. Atmos. Environ. 45, 802–807.
Pirjola, L., Paasonen, P., Pfeiffer, D., Hussein, T., Hameri, K., Koskentalo, T., Virtanen, A., Ronkko, T., Keskinen, J., Pakkanen, T.A., Hillamo, R.E., 2006. Dispersion of particles and trace gases nearby a city highway: mobile laboratory measurements in Finland. Atmos. Environ. 40, 867–879.
Polo Rehn L. (2013). Caractérisation et impacts des émissions de polluants du transport routier: apports méthodologiques et cas d'études en Rhône-Alpes. In: France, <http://tel.archives-ouvertes.fr/tel-00876623>.
Polo Rehn, L., Waked, A., Charron, A., Piot, C., Besombes, J.L., Marchand, N., Guillaud, G., Favez, O., Jaffrezo, J.L., 2014. Estimation de la contribution des émissions véhiculaires à l'échappement et hors échappement aux teneurs atmosphériques en PM10 par Positive Matrix Factorization (PMF). Pollut. Atmos. 221, 2268–3798.
Qian, W., Venkatram, A., 2011. Performance of steady-state dispersion models under low wind-speed conditions. Boundary-Layer Meteorol. 138, 475–491.
Sportisse, B., 2009. Fundamentals in Air Pollution: From Processes to Modeling. Springer.
Venkatram, A., Snyder, M., Isakov, V., 2013. Modeling the impact of roadway emissions in light wind, stable and transition conditions. Transport. Res. D 24, 110–119.
Wang, Y.J., Zhang, K.M., 2009. Modeling near-road air quality using a computational fluid dynamics model, CFD-VIT-RIT. Environ. Sci. Technol. 43, 7778–7783.
Yu, S., Eder, B., Dennis, R., Chu, S.H., Schwartz, S.E., 2006. New unbiased symmetric metrics for evaluation of air quality models. Atmos. Sci. Lett. 7, 26–34.
Zannetti, P., 1990. Air Pollution Modelling: Theories, Computational Methods, and Available Software. Computational Mechanics Publications.
Zhang, K., Batterman, S., 2010. Near-road air pollutant concentrations of CO and PM2.5: a comparison of MOBILE6.2/CALINE4 and generalized additive models. Atmos. Environ. 44, 1740–1748.